Supporting information for:

Long wavelength excitable near-infrared fluorescent nanoparticles with aggregation-induced emission characteristics for image-guided tumor resection

Jie Liu,[1] Chao Chen,[2] Shenglu Ji,[2] Qian Liu,[3] Dan Ding,*[4] Zhao[1] and Bin Liu*[1]*

[1]Department of Chemical and Biomolecular Engineering, 4 Engineering Drive 4, National University of Singapore, 117585, Singapore

[2]State Key Laboratory of Medicinal Chemical Biology, Key Laboratory of Bioactive Materials, Ministry of Education, and College of Life Sciences, Nankai University, Tianjin 300071, P. R. China

[3]Department of Urology, Tianjin First Central Hospital, Tianjin 300192, P. R. China

Corresponding Authors

*E-mail: cheliub@nus.edu.sg (B. L), dingd@nankai.edu.cn (D. D.), simonlq@163.com (Q. L.).

Experimental Section

General materials. Dulbecco's modified eagle's medium (DMEM) was a commercial product of National University Medical Institutes (Singapore). 1,2-Distearoyl-*sn*-glycero-3-phosphoethanolamine-*N*-[methoxy(polyethylene glycol)-2000] (DSPE-PEG_{2000}) was obtained from Avanti Polar Lipids, Inc. 10 × phosphate buffered saline (PBS) with pH = 7.4 (ultrapure grade) is commercially available from 1st BASE Singapore. MilliQ water (18.2 MQ) was used for all the experiments requiring aqueous medium. All other chemicals and reagents used in this study were purchased from Sigma-Aldrich and used as received unless specified otherwise.

Characterization. Nuclear magnetic resonance (NMR) spectra were performed on a Bruker Avance 400 NMR spectrometer (400 MHz for ^1H, referenced to TMS at δ = 0.00 ppm and 100 MHz for ^{13}C, referenced to $CDCl_3$ at 77.0 ppm). The average particle size and size distribution of

nanoparticles were recorded by laser light scattering (LLS) using Brookhaven instruments corporation (BIC) 90 plus (λ = 659 nm). Transmission electron microscopy (TEM) studies were performed on a JEOL JEM-2010 electron microscope with an accelerating voltage of 200 KV. UV–vis spectra were measured on a Shimadzu UV-1700 spectrometer. Photoluminescence (PL) spectra were collected on a Perkin Elmer LS-55 equiped with a xenon lamp excitation source and a Hamamatsu (Japan) 928 PMT, using 90 degree angle detection for solution samples. All UV-vis and PL spectra were measured at 24 ± 1 ^{o}C. Fluorescence quantum yield was determined using IR-125 in dimethyl sulfoxide (13%) as the standard. The absorbance of solutions was kept below 0.1 to avoid internal filter effect. Confocal laser-scanning microscopy (CLSM) images were collected on a Zeiss LSM 410 (jena, Germany) CLSM with imaging soft (Fluoview FV1000). X-ray diffraction (XRD) patterns were collected on a Bruker's X-ray powder diffractometer (D8 Advance, Cu, Kα, λ = 0.154 nm). Matrix-assisted laser desorption and ionization time-of-fight mass spectrometry (MALDI-TOF-MS) measurements were performed on a Bruker's autoflex speed equipment, using 2,5-dihydroxybenzoic acid as matrix.

Preparation of nanoaggregates. Stock solutions of the NIR fluorescent compounds in tetrahydrofuran (THF) were prepared with a concentration of 5×10^{-4} M. Aliquots of the stock solutions were added to 10 mL volumetric flasks and diluted with appropriate amounts of THF, then water was added in one portion under vigorous stirring to afford 5×10^{-6} M solutions with different water fractions (0–90 vol%). The PL measurements of the resultant mixture solutions were carried out immediately upon excitation at 630 nm.

Fabrication of AIE NPs. A mixture of AIE molecules (1 mg) and DSPE-PEG_{2000} (2 mg) dissolved well in THF (1 mL) was added into water (10 mL), followed by sonication for 2 min using a microtip sonicator at 16 W output (XL2000, Misonix Incorporated, NY). After the mixture was

stirred vigorously for 24 h to evaporate THF, filtration was performed using a 0.2 μm syringe driven filter to yield the corresponding AIE NPs for further use.

Cell Culture. Luciferase-expressed 4T1 breast cancer cells and L02 hepatic cells were cultured in Dulbecco's Modified Eagle's Medium (DMEM) containing 10% FBS and 1% penicillin-streptomycin at 37 ^{o}C in a humidified environment containing 5% CO_2, respectively. Before experiments, the cells were precultured until confluence was reached.

Cell Imaging. 4T1 cancer cells were cultured in confocal imaging chambers at 37 ^{o}C. AIE NPs (2 nM) in FBS-free culture medium were added to the chamber. After incubation for 2 h, the cells were washed with 1 × PBS buffer and then fixed with 4% paraformaldehyde. After stainingwith DAPI for 10 min, the cells were imaged by confocal laser scanning microscope (Zeiss LSM 410, Jena, Germany). The fluorescent signal from AIE NPs was collected from 700 to 800 nm upon excitation at 633 nm.

Cytotoxicity Study. MTT assays were employed to evaluate the cytotoxicities of AIE NPs against both cancer and normal cells. In brief, 4T1 cancer cells and L02 hepatic cells were seeded in 96-well plates (Costar, IL, USA) at a density of 4 × 10^4 cells/mL, respectively. After 24 h incubation, both cells were exposed to a series of doses of AIE NPs. At 48 h post addition of AIE NPs, the wells were washed with 1 × PBS buffer and 100 μL of freshly prepared MTT solution (0.5 mg/mL) in culture medium was added into each well. The MTT medium solution was carefully removed after 3 h incubation in the incubator. DMSO (100 μL) was then added into each well and the plate was gently shaken for 10 min at room temperature to dissolve all the precipitates formed. The absorbance of MTT at 490 nm was then monitored by the microplate Reader (GENios Tecan). Cell viability was expressed by the ratio of the absorbance of cells incubated with AIE NPs to that of the cells incubated with culture medium only.

Animals and Tumor Models. All animal studies were performed in compliance with the guidelines set by Tianjin Committee of Use and Care of Laboratory Animals and the overall project protocols were approved by the Animal Ethics Committee of Nankai University. All the mice were purchased from Laboratory Animal Center of the Academy of Military Medical Sciences (Beijing, China). To set up peritoneal carcinomatosis-bearing mouse model, a total of 300,000 luciferase-expressed 4T1 cancer cells in 0.1 mL of PBS buffer were intraperitoneally injected into the Balb/c mice. After 5 days, small tumor nodules were formed and scattered in the mouse peritoneal cavity, which could be detected by bioluminescence imaging upon injection of a solution of D-luciferin (150 mg/kg).

Study on Evaluation of *In Vivo* Toxicity. Healthy BALB/c mice were randomly assigned to 2 groups and each group contained 4 mice. On day 0, the mice in one group were intravenously injected with 100 μL of AIE NPs (100 nM). After the injection, 9 day follow-up experiments were conducted, in which the weights of all the mice in two groups were scrutinized. On day 9, the mice in two groups were sacrificed and the blood was collected through cardiac puncture at the time of sacrifice for blood chemistry analyses by Tianjin First Central Hospital.

Surgery with AIE NP Fluorescence Guidance. The mice bearing peritoneal carcinomatosis were intravenously injected with 100 μL of AIE NPs (50 nM). At 24 h post-injection, the mice were anesthetized. The abdomen or thoracic cavity of mice was opened, followed by bioluminescence and fluorescence imaging during surgery. The excised tumor nodules were analyzed by both imaging modalities. Alternatively, the surgery was performed by the experience of a surgeon without imaging guidance (unguided). Bioluminescence imaging was performed using the Xenogen IVIS® Lumina II system post intraperitoneal injection of D-luciferin (150 mg/kg) into the mice. The bioluminescence signals were quantified in units of maximum photons per second

per square centimeter per steridian. On the other hand, fluorescence imaging was carried out using a Maestro EX *in vivo* fluorescence imaging system (CRi, Inc.). The light with a central wavelength at 635 nm was selected as the excitation source. *In vivo* spectral imaging from 670 nm to 900 nm in 10 nm steps was conducted with an exposure time of 150 ms for each image frame. The original fluorescence images contained both signal and mouse autofluorescence were shown, which were not post-processed by any softwares such as unmixing function of Maestro software to remove the background fluorescence.

Statistical Analysis. Quantitative data were expressed as mean ± standard deviation. Statistical comparisons were made by ANOVA analysis and Student's *t*-test. P value < 0.05 was considered statistically significant.

Synthesis of *α*-DTPEBBTD-Cx and *β*-DTPEBBTD-Cx

(4-Bromophenyl)(4-methoxyphenyl)methanone (1). To a solution of 4-bromobenzoyl chloride (2.17 g, 10.0 mmol) and aluminum chloride (1.36 g, 10.2 mmol) in dry dichloromethane (15 mL) under argon atmosphere was added anisole (3.26 mL, 30 mmol) in an ice bath. The mixture was kept at 0~10 ^{o}C for 1 h and then stirred at room temperature overnight. Hydrochloric acid aqueous solution (100 mL, 1 M) was carefully added into the reaction mixture in ice bath to yield precipitates. After filtration under reduced pressure, the obtained solid was further purified by silica gel column chromatography using a mixture of hexane/ethyl acetate (9/1) as eluent to give (4-bromophenyl)(4-methoxyphenyl)methanone as a white solid. ^{1}H NMR (400 MHz, $CDCl_3$, ppm) δ 7.81–7.78 (m, 2 H), 7.65–7.62 (m, 4 H), 6.98–6.95 (m, 2 H), 3.89 (s, 3 H). ^{13}C NMR (100 MHz, $CDCl_3$, ppm) δ 194.5, 163.6, 137.2, 132.6, 131.6, 131.4, 129.9, 127.0, 113.8, 55.7.

1-(4-Bromophenyl)-2,2-diphenyl-1-(4-methoxyphenyl)ethene (2). Diphenylmethane (2.02 g, 12.0 mmol) in anhydrous THF (50 mL) was stirred at 0 °C under argon atmosphere, then *n*-BuLi (1.6 M in hexane, 6.87 mL, 11.0 mmol) was added dropwise into the mixture. The resultant red mixture was kept at 0 °C for 1 h, then a solution of compound **1** (2.91 g, 10 mmol) in anhydrous THF (10 mL) was added slowly. The reaction mixture was stirred at room temperature overnight. After treatment with a saturated NH_4Cl aqueous solution, the crude product was extracted with dichloromethane (50 mL × 3). The combined organic phase was sequentially washed with water, dried over $MgSO_4$ and filtered. After solvent removal, the residue and *p*-toluenesulfonic acid (86.0 mg, 0.5 mmol) were treated in toluene (25 mL) at 100 °C for 3 h. The crude product was sequentially extracted with dichloromethane (50 mL × 3), washed with water (100 mL × 3), and dried over $MgSO_4$. After solvent removal, the residue was purified by silica gel column chromatography (hexane/dichloromethane/ethyl acetate = 8/2/0.2) to yield compound **2** as a white solid (3.48 g, yield: 79%). ^{1}H NMR (400 MHz, $CDCl_3$, ppm) δ 7.23–7.22 (m, 2 H), 7.14–7.10 (m, 6 H), 7.04–7.01 (m, 4 H), 6.93–6.90 (m, 4 H), 6.66–6.64 (m, 2 H), 3.75 (s, 3 H). ^{13}C NMR (100 MHz, $CDCl_3$, ppm) δ 158.38, 143.86, 143.71, 143.11, 140.85, 139.37, 135.71, 133.17, 132.64, 131.41, 131.36, 130.93, 127.97, 127.88, 126.65, 126.56, 120.49, 113.31, 55.24.

2,2-Diphenyl-1-(4-bromophenyl)-1-(4-hydroxyphenyl)ethene (3). To a solution of compound **2** (3.53 g, 8.0 mmol) in anhydrous dichloromethane (20 mL) under argon atmosphere was slowly added boron tribromide solution (1 M in dichloromethane, 10.5 mL, 10.5 mmol) at –78 °C. Then the reaction mixture was stirred at room temperature overnight. After quenching with ice water, the crude product was sequentially extracted with dichloromethane (50 mL × 3), washed with water (100 mL × 3), dried over Na_2SO_4 and filtered. After solvent removal, the residue was purified by silica gel column chromatography (hexane/dichloromethane = 3/7) to afford compound **3** as a

light green solid (2.0 g, yield: 91%). ^{1}H NMR (400 MHz, $CDCl_3$, ppm) δ 7.23–7.20 (m, 2 H), 7.13–7.09 (m, 6 H), 7.02–6.99 (m, 4 H), 6.59–6.55 (m, 2 H), 4.58 (s, 1 H). ^{13}C NMR (100 MHz, $CDCl_3$, ppm) δ 154.42, 143.83, 143.64, 143.00, 140.90, 139.32, 135.84, 133.14, 132.82, 131.38, 131.33, 130.93, 127.96, 127.87, 126.67, 126.56, 120.51, 114.88.

2,2-Diphenyl-1-(4-bromophenyl)-1-(4-butoxyphenyl)ethene (4a). To a mixture of compound **3** (852.0 mg, 2.0 mmol) and cesium carbonate (Cs_2CO_3, 975.0 mg, 3.0 mmol) in anhydrous dimethylformamide (DMF, 5.0 mL) was added 1-bromobutane (0.32 mL, 3.0 mmol) under argon atmosphere. The reaction mixture was stirred at room temperature overnight. After quenching with water, the crude product was sequentially extracted with dichloromethane (30 mL × 3), washed with water (50 mL × 3), and dried over $MgSO_4$. After solvent removal, the residue was further purified by silica gel column chromatography (hexane/dichloromethane = 9/1) to give compound **4a** as a light green fibrous solid (888.6 mg, yield: 92%). ^{1}H NMR (400 MHz, $CDCl_3$, ppm) δ 7.25–7.23 (m, 2 H), 7.14–7.10 (m, 6 H), 7.06–7.01 (m, 4 H), 6.94–6.90 (m, 4 H), 6.67–6.62 (m, 2 H), 3.91 (t, J = 8 Hz, 2 H), 1.76 (m, 2 H), 1.50 (m, 2 H), 0.98 (t, J = 8 Hz, 3 H). ^{13}C NMR (100 MHz, $CDCl_3$, ppm) δ 158.00, 143.90, 143.76, 143.15, 140.72, 139.45, 135.46, 133.20, 132.61, 131.42, 131.36, 130.91, 127.96, 127.87, 126.62, 126.52, 120.47, 113.83, 67.64, 31.49, 19.40, 14.04.

2,2-Diphenyl-1-(4-octyloxyphenyl)-1-(4-bromophenyl)ethene (4b). Compound **4b** was obtained as viscous oil (948.6 mg, yield: 88%) using a similar synthetic procedure as compound **4a**, starting from compound **3** (854.0 mg, 2.0 mmol), Cs_2CO_3 (975.0 mg, 3.0 mmol), DMF (5.0 mL) and 1-bromooctane (0.52 mL, 3 mmol). ^{1}H NMR (400 MHz, $CDCl_3$, ppm) δ 7.24–7.20 (m, 2 H), 7.14–7.10 (m, 6 H), 7.05–7.00 (m, 4 H), 6.92–6.89 (m, 4 H), 6.66–6.62 (m, 2 H), 3.88 (t, J = 8 Hz, 2 H), 1.75 (m, 2 H), 1.44 (m, 2 H), 1.36–1.30 (m, 8 H), 0.90 (t, J = 8 Hz, 3 H). ^{13}C NMR (100 MHz, $CDCl_3$, ppm) δ 158.04, 143.93, 143.79, 143.18, 140.76, 139.50, 135.49, 133.20,

132.62, 131.43, 131.37, 130.92, 127.97, 127.88, 126.63, 126.53, 120.48, 113.88, 68.02, 31.96, 29.52, 29.44, 29.36, 26.20, 22.80, 14.23.

1,2-Diphenyl-2-(4-methoxyphenyl)-1-(4-trimethylstannylphenyl)ethane (5a). To a solution of compound **2** (441.0 mg, 1.0 mmol) in anhydrous THF (10 mL) at –78 °C under argon atmosphere was slowly added *n*-BuLi (1.6 M in hexane, 0.93 mL, 1.5 mmol). After the reaction mixture was stirred at –78 °C for 1.5 h, trimethyltin chloride (Me_3SnCl, 1.0 M in THF, 1.8 mL) was added to the mixture in one portion. Then it was slowly warmed to room temperature and stirred overnight. The mixture was poured into water and extracted with dichloromethane (30 mL × 3). The combined organic layer was sequentially washed with water (100 mL × 3), dried over Na_2SO_4, and filtered. After solvent removal, the residue was obtained as colorless liquid and used directly in the next step without further purification.

2-(4-Butoxyphenyl)-1,2-diphenyl-1-(4-trimethylstannylphenyl)ethane (5b). Compound **5b** was synthesized using a similar synthetic procedure as compound **5a**, starting from compound **4a** (483.0 mg, 1.0 mmol), *n*-BuLi (1.6 M in hexane, 0.93 mL, 1.5 mmol), Me_3SnCl (1.0 M in THF, 1.8 mL) and anhydrous THF (15 mL). The obtained colorless liquid was used directly in the next step without further purification.

1,2-Diphenyl-2-(4-octyloxyphenyl)-1-(4-trimethylstannylphenyl)ethane (5c). Compound **5c** was synthesized using a similar synthetic procedure as compound **5a**, starting from compound **4b** (539.0 mg, 1.0 mmol), *n*-BuLi (1.6 M in hexane, 0.93 mL, 1.5 mmol), Me_3SnCl (1.0 M in THF, 1.8 mL) and anhydrous THF (15 mL). The obtained colorless liquid was used directly in the next step without further purification.

***α*-DTPEBBTD-C1**. A solution of compound **5a** (210.0 mg, 0.4 mmol), 4,8-dibromobenzo[1,2-*c*:4,5-*c*′]bis([1,2,5]thiadiazole) (BBTD, 35.2 mg, 0.1 mmol) and $Pd(PPh_3)_4$ (11.5 mg, 10 μmol) in toluene (30 mL) was heated at 100 °C under argon atmosphere for 36 h. After cooling to room temperature, the mixture was sequentially diluted with dichloromethane (200 mL), washed with water (200 mL × 3) and dried over $MgSO_4$. After solvent removal, the residue was purified by silica gel column chromatography (hexane/dichloromethane = 4/6) to afford *α*-DTPEBBTD-C1 as a blue solid (29 mg, yield: 32%). Due to the poor solubility of α-BTPEBBTD in the NMR solvent, the ^{13}C NMR spectrum of **11a** was not obtained. ^1H NMR (400 MHz, $CDCl_3$, ppm) δ 8.07 (d, *J* = 8 Hz, 4 H), 7.30 (d, *J* = 8 Hz, 4 H), 7.15–7.05 (m, 24 H), 6.68 (d, *J* = 8 Hz, 4 H), 3.76 (s, 6 H).

***α*-DTPEBBTD-C4**. Compound *α*-DTPEBBTD-C4 was obtained as blue solid (55 mg, yield: 56%%) using a similar synthetic procedure as compound *α*-DTPEBBTD-C1, starting from compound **5b** (226.8 mg, 0.4 mmol), BBTD (35.2 mg, 0.1 mmol) and $Pd(PPh_3)_4$ (11.5 mg, 10 μmol) in toluene (30 mL). ^1H NMR (400 MHz, $CDCl_3$, ppm) δ 8.06 (d, J = 8 Hz, 4 H), 7.30 (d, J = 8 Hz, 4 H), 7.16–7.08 (m, 20 H), 7.06 (d, *J* = 8 Hz, 4 H), 6.69 (d, *J* = 8 Hz, 4 H), 3.91 (t, *J* = 8 Hz, 4 H), 1.74 (t, *J* = 8 Hz, 4 H), 1.50–1.44 (m, 4 H), 0.97 (t, *J* = 8 Hz, 6 H). ^{13}C NMR (100 MHz, $CDCl_3$, ppm) δ 158.01, 152.91, 144.80, 144.29, 144.08, 141.11, 140.39, 135.96, 133.28, 132.90, 131.63, 131.56, 131.51, 131.32, 127.97, 127.85, 126.64, 126.46, 121.11, 113.88, 67.69, 31.54, 19.41, 14.02.

***α*-DTPEBBTD-C8**. Compound *α*-DTPEBBTD-C8 was obtained as blue solid (61 mg, yield: 59%) using a similar synthetic procedure as compound *α*-DTPEBBTD-C1, starting from compound **5c** (249.2 mg, 0.4 mmol), BBTD (35.2 mg, 0.1 mmol) and $Pd(PPh_3)_4$ (11.5 mg, 10 μmol) in toluene (30 mL). ^1H NMR (400 MHz, $CDCl_3$, ppm) δ 8.06 (d, *J* = 8 Hz, 4 H), 7.30 (d, *J* = 8 Hz, 4 H), 7.15–7.08 (m, 20 H), 7.05 (d, *J* = 8 Hz, 4 H), 6.68 (d, *J* = 8 Hz, 4 H), 3.89 (t, *J* = 8 Hz, 4 H), 1.78–1.71

(m, 4 H), 1.44 (m, 4 H), 1.33–1.28 (m, 16 H), 0.89 (t, J = 8 Hz, 6 H). ^{13}C NMR (100 MHz, $CDCl_3$, ppm) δ 158.01, 152.92, 144.81, 144.30, 144.09, 141.11, 140.40, 135.96, 133.28, 132.90, 131.63, 131.56, 131.51, 131.33, 127.97, 127.85, 126.64, 126.46, 121.12, 113.90, 68.04, 31.96, 29.53, 29.48, 29.37, 26.22, 22.80, 14.23.

1-(4-Bromophenyl)-2-(4-methoxyphenyl)-1,2-diphenylethane (6). A two-necked round-bottom flask with a reflux condenser was charged with 4-bromobenzophenone (3.91 g, 15.0 mmol), 4-methoxybenzophenone (3.18 g, 15.0 mmol) and zinc (5.20 g, 80.0 mmol). The flask was degassed with three freeze-pump-thaw cycles to remove air, and then anhydrous THF (150 mL) was added. The mixture was cooled to –78 °C and $TiCl_4$ (4.9 mL, 45.0 mmol) was added dropwise by a syringe. The reaction mixture was slowly warmed to room temperature and stirred for 0.5 h before it was heated to 80 °C for 24 h. After cooling down to room temperature, the reaction was quenched by the addition of 10% K_2CO_3 aqueous solution (100 mL). The mixture was filtered off to remove insoluble materials and washed with dichloromethane (150 mL). The organic layer was dried over $MgSO_4$ and filtered. After solvent removal, the residue was further purified by silica gel column chromatography (hexane/dichloromethane/ethyl acetate = 8/2/0.1) to give compound **6** as a light green solid (3.79 g, yield: 57%). ^{1}H NMR (400 MHz, $CDCl_3$, ppm): δ 7.15–7.38 (m, 2 H), 7.33–7.28 (m, 2 H), 7.16–7.10 (m, 4 H), 7.06–7.01 (m, 4 H), 6.99–6.91 (m, 4 H), 6.74–6.67 (m, 2 H), 3.73 (d, 3 H). ^{13}C NMR (100 MHz, $CDCl_3$, ppm): δ 158.3, 143.6, 143.0, 141.2, 135.6, 133.0, 132.5, 132.4, 131.4, 131.3, 130.9, 130.8, 130.1, 128.4, 128.3, 127.8, 127.7, 127.6, 126.5, 126.4, 120.2, 113.0, 55.6, 55.0.

1-(4-Bromophenyl)-2-(4-hydroxyphenyl)-1,2-diphenylethane (7). Compound **7** was obtained as a light green solid (3.13 g, yield: 92%) using a procedure similar to that used for compound **3**, starting from compound **6** (2.2 g, 5.0 mmol) and BBr_3 solution (1 M in dichloromethane, 7 mL,

7.0 mmol). ^{1}H NMR (400 MHz, $CDCl_3$, ppm): δ 7.25–7.19 (m, 2 H), 7.14–6.98 (m, 10 H), 6.92–6.86 (m, 4 H), 6.60–6.55 (m, 2 H), 4.88 (d, 1H). ^{13}C NMR (100 MHz, $CDCl_3$, ppm): δ 153.66, 153.55, 142.93, 142.88, 142.85, 142.35, 142.26, 140.47, 138.24, 138.20, 135.38, 135.27, 132.36, 132.06, 132.04, 130.64, 130.27, 130.17, 127.22, 127.11, 127.02, 126.04, 125.94, 125.87, 119.63, 114.18, 113.99.

1-(4-Bromophenyl)-2-(4-butoxyphenyl)-1,2-diphenylethane (8a). Compound **8a** was obtained as a fibrous solid (927 mg, yield: 96%) using a similar synthetic procedure as compound **4a**, starting from compound **7** (854.0 mg, 2.0 mmol), Cs_2CO_3 (975.0 mg, 3.0 mmol), DMF (5.0 mL) and 1-bromobutane (0.32 mL, 3.0 mmol). ^{1}H NMR (400 MHz, $CDCl_3$, ppm): δ 7.28–7.21 (m, 2 H), 7.14–7.01 (m, 10 H), 6.95–6.87 (m, 4 H), 6.69–6.64 (m, 2 H), 3.93–3.88 (m, 2 H), 1.79–1.73 (m, 2 H), 1.54–1.47 (m, 2 H), 1.01–0.97 (m, 3 H). ^{13}C NMR (100 MHz, $CDCl_3$, ppm): δ 157.90, 157.80, 143.67, 143.60, 143.56, 143.47, 143.04, 142.98, 141.26, 138.63, 138.58, 135.39, 132.98, 132.43, 132.41, 132.38, 131.30, 131.27, 131.02, 130.91, 130.86, 130.75, 127.81, 127.70, 127.58, 126.48, 126.41, 120.45, 120.18, 113.78, 113.74, 113.57, 67.48, 67.44, 31.34, 31.32, 19.24, 13.89, 13.87.

1-(4-Bromophenyl)-2-(4-butoxyphenyl)-1,2-diphenylethane (8b). Compound 8**b** was synthesized using a similar synthetic procedure as compound **4a**, starting from compound **7** (852.0 mg, 2 mmol), Cs_2CO_3 (975.0 mg, 3 mmol), DMF (5.0 mL) and 1-bromooctane (0.52 mL, 3 mmol). The crude product was purified by silica gel column chromatography (hexane/dichloromethane = 9/1) to give compound **8b** as a light green fibrous solid (1.0 g, yield: 93%). ^{1}H NMR (400 MHz, $CDCl_3$, ppm): δ 7.28–7.24 (m, 2 H), 7.17–7.04 (m, 10 H), 6.98–6.91 (m, 4 H), 6.71–6.66 (m, 2 H), 3.95–3.90 (m, 2 H), 1.82–1.75 (m, 2 H), 1.48–1.44 (m, 2 H), 1.36–1.33 (m, 8 H), 0.95–0.93 (m, 3 H). ^{13}C NMR (100 MHz, $CDCl_3$, ppm): δ 157.92, 157.83, 143.70, 143.63, 143.59, 143.50, 143.01,

141.28, 138.62, 135.53, 133.02, 132.49, 132.46, 132.43, 131.39, 131.33, 131.30, 130.89, 130.78, 127.84, 127.80, 127.72, 127.69, 127.61, 127.57, 126.61, 126.51, 126.43, 120.19, 113.77, 113.60, 67.91, 67.82, 31.82, 29.40, 29.38, 29.31, 29.30, 29.24, 29.23, 26.08, 26.07, 22.66, 14.12.

Compounds 9a–c. Compounds 9a–c were synthesized using a similar procedure as compounds 5a–c, and used directly without further purification.

***β*-DTPEBBTD-C1**. Compound *β*-DTPEBBTD-C1 was obtained as blue solid (38.4 mg, yield: 42%) using a similar synthetic procedure as compound *α*-DTPEBBTD-C1, starting from compound **9a** (210.0 mg, 0.4 mmol), BBTD (35.2 mg, 0.1 mmol) and $Pd(PPh_3)_4$ (11.5 mg, 10 μmol) in toluene (30 mL). ^{1}H NMR (400 MHz, $CDCl_3$, ppm) δ 8.09–8.03 (m, 4 H), 7.33–7.29 (m, 4 H), 7.16–6.98 (m, 24 H), 6.73–6.66 (m, 4 H), 3.76 (s, 0.85), 3.73 (s, 5.15). ^{13}C NMR (100 MHz, $CDCl_3$, ppm) δ 158.52, 152.87, 144.77, 144.16, 144.02, 141.63, 139.84, 136.18, 133.16, 132.80, 131.74, 131.58, 131.45, 131.40, 127.98, 127.86, 127.74, 126.60, 126.52, 121.03, 113.46, 55.25.

***β*-DTPEBBTD-C4**. Compound *β*-DTPEBBTD-C4 was obtained as blue solid (50.8 mg, yield: 51%) using a similar synthetic procedure as compound *α*-DTPEBBTD-C1, starting from compound **9b** (226.8 mg, 0.4 mmol), BBTD (35.2 mg, 0.1 mmol) and $Pd(PPh_3)_4$ (11.5 mg, 10 μmol) in toluene (30 mL). ^{1}H NMR (400 MHz, $CDCl_3$, ppm) δ 8.10–8.02 (m, 4 H), 7.34–7.27 (m, 4 H), 7.23–7.09 (m, 22 H), 7.00–6.98 (d, J = 8 Hz, 2 H), 6.73–6.66 (m, 4 H), 3.93–3.88 (m, 4 H), 1.77–1.70 (m, 4 H), 1.52–1.44 (m, 4 H), 1.01–0.92 (m, 6 H). ^{13}C NMR (100 MHz, $CDCl_3$, ppm) δ 158.11, 157.93, 152.83, 152.80, 152.77, 144.81, 144.80, 144.73, 144.20, 144.14, 144.07, 144.06, 141.70, 139.70, 136.06, 135.93, 133.10, 133.07, 132.77, 132.72, 131.74, 131.71, 131.64, 131.59, 131.43, 131.40, 131.33, 127.95, 127.84, 127.70, 126.76, 127.57, 126.48, 120.99, 120.95, 120.92, 113.98, 113.72, 67.63, 31.50, 31.46, 19.38, 19.36, 14.00, 13.98.

***β*-DTPEBBTD-C8**. Compound *β*-DTPEBBTD-C8 was obtained as a blue solid (59.9 mg, yield: 54%) using a similar synthetic procedure as compound *α*-DTPEBBTD-C1, starting from compound **9c** (249.2 mg, 0.4 mmol), BBTD (35.2 mg, 0.1 mmol) and $Pd(PPh_3)_4$ (11.5 mg, 10 μmol) in toluene (30 mL). ^{1}H NMR (400 MHz, $CDCl_3$, ppm) δ 8.10–8.02 (m, 4 H), 7.33–7.27 (m, 4 H), 7.21–7.08 (m, 22 H), 6.99–6.97 (d, *J* = 8 Hz, 2 H), 6.72–6.65 (m, 4 H), 3.92–3.86 (m, 4 H), 1.78–1.71 (m, 4 H), 1.33–1.26 (m, 20 H), 0.93–0.85 (m, 6 H). ^{13}C NMR (100 MHz, $CDCl_3$, ppm) δ 158.12, 157.94, 152.91, 152.86, 152.83, 144.82, 144.76, 144.22, 144.16, 144.08, 141.72, 139.70, 136.07, 135.93, 133.13, 133.10, 132.78, 132.74, 131.77, 131.73, 131.66, 131.61, 131.43, 131.32, 127.97, 127.85, 127.71, 126.76, 126.58, 126.49, 125.65, 121.03, 113.98, 113.73, 67.98, 31.95, 31.91, 30.48, 29.52, 29.49, 29.45, 29.43, 29.37, 29.33, 26.21, 26.19, 22.80, 22.75, 14.24, 14.21.

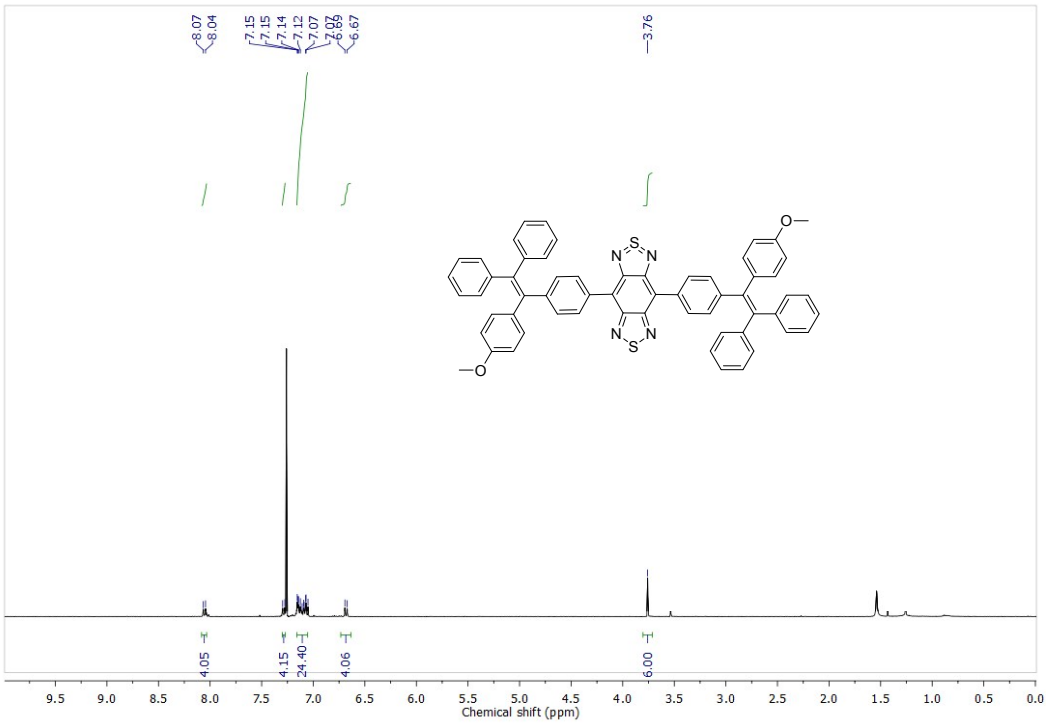

Fig. S1 ^{1}H NMR spectrum of *α*-DTPEBBTD-C1 in $CDCl_3$.

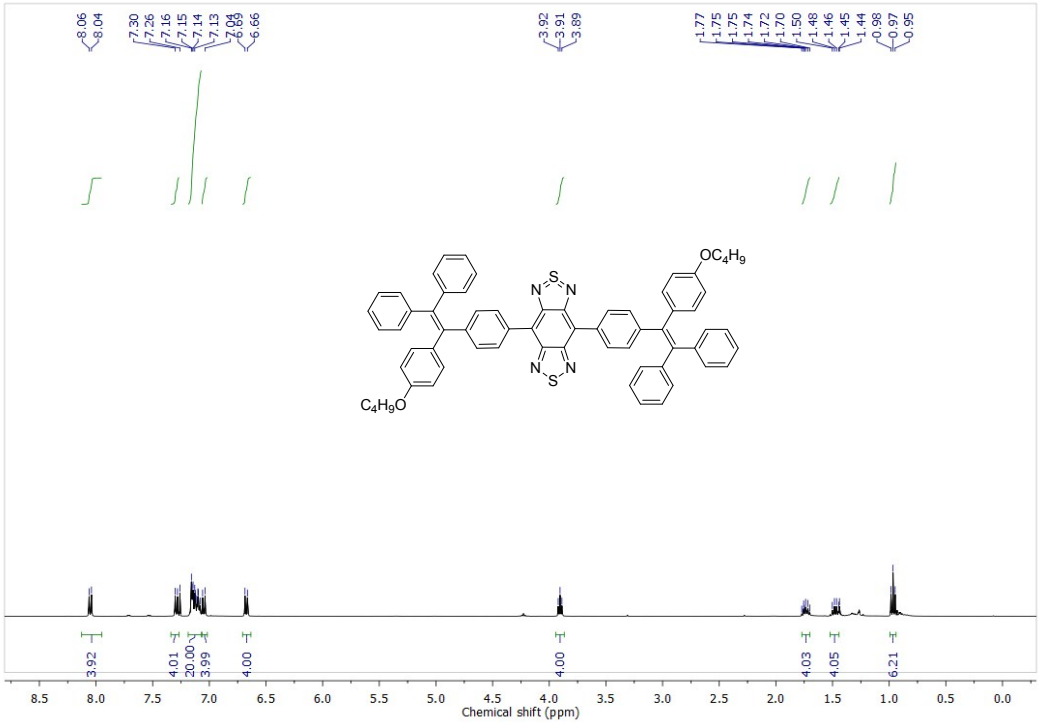

Fig. S2 ^{1}H NMR spectrum of *α*-DTPEBBTD-C4 in $CDCl_3$.

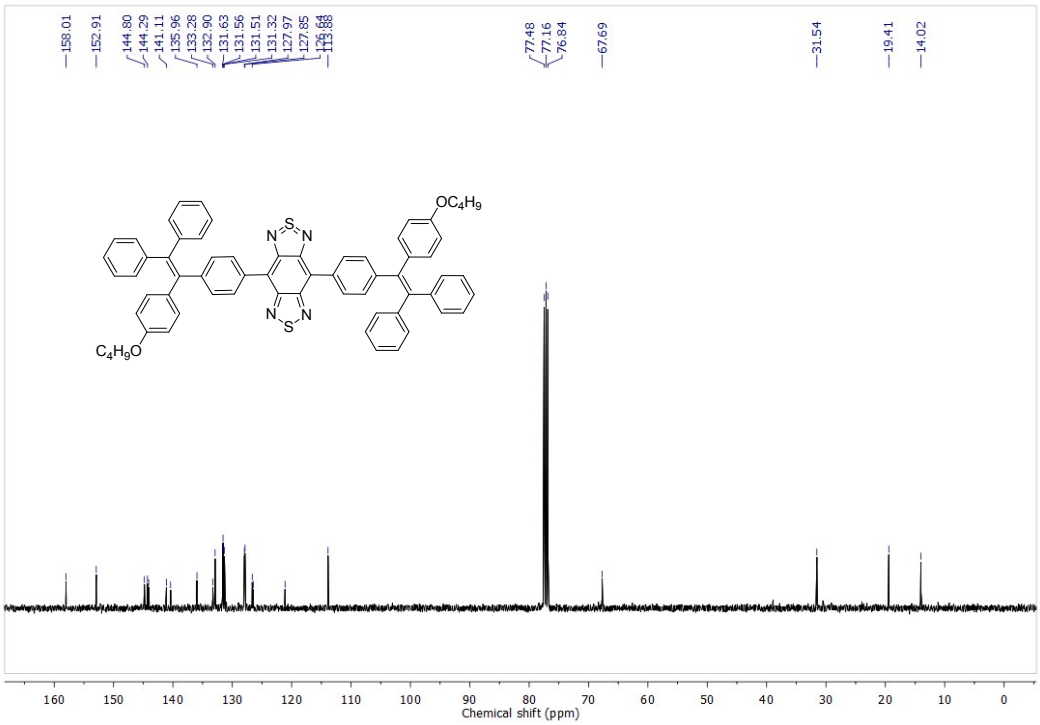

Fig. S3 ^{13}C NMR spectrum of α-DTPEBBTD-C4 in $CDCl_3$.

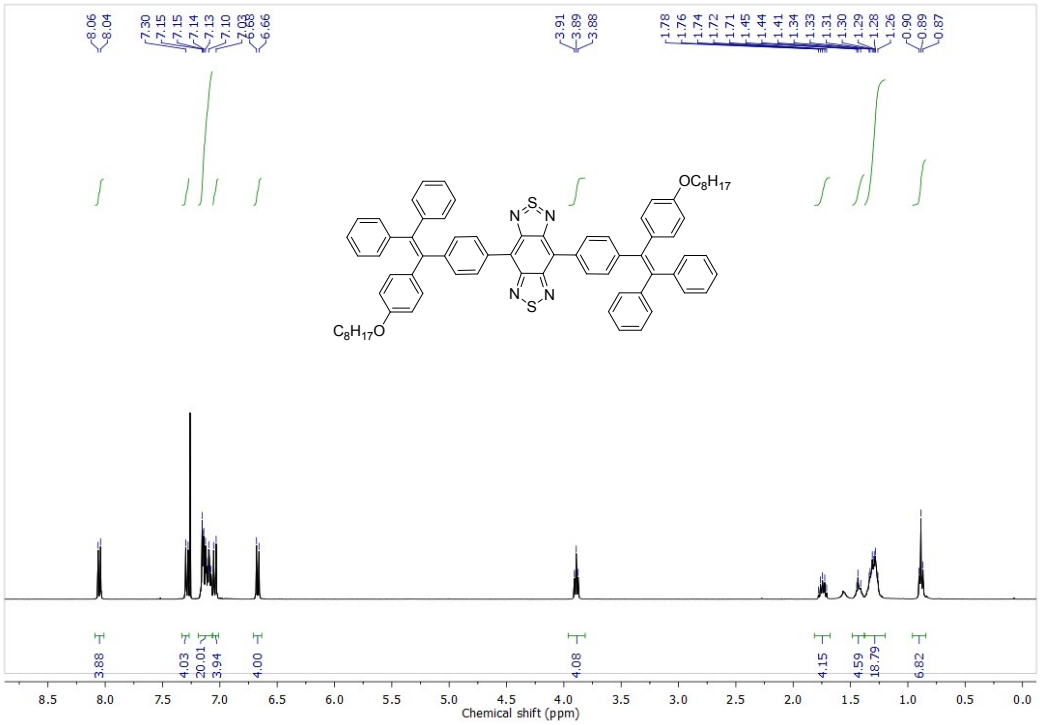

Fig. S4 ^{1}H NMR spectrum of α-DTPEBBTD-C8 in $CDCl_3$.

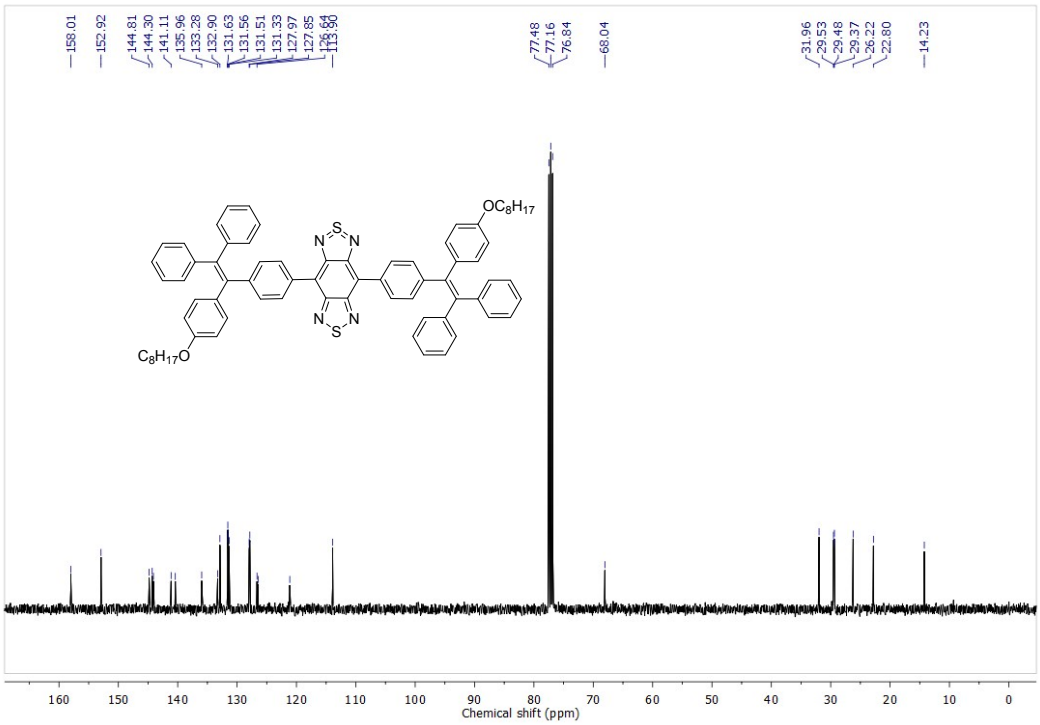

Fig. S5 ^{13}C NMR spectrum of α-DTPEBBTD-C8 in $CDCl_3$.

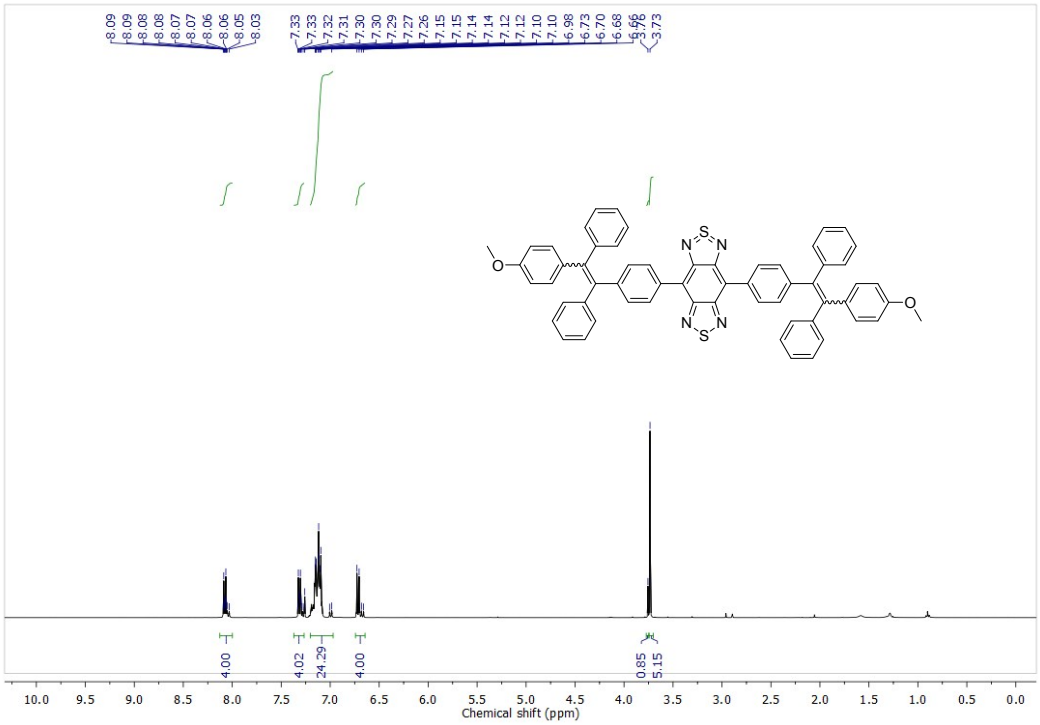

Fig. S6 ^{1}H NMR spectrum of β-DTPEBBTD-C1 in $CDCl_3$.

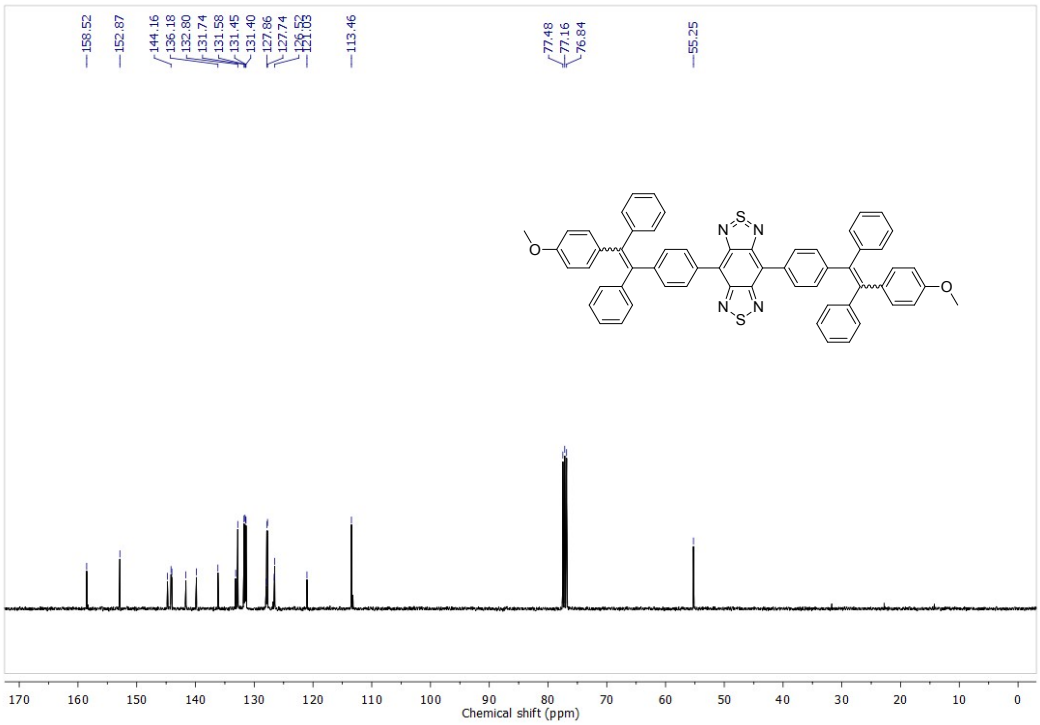

Fig. S7 ^{13}C NMR spectrum of *β*-DTPEBBTD-C1 in $CDCl_3$.

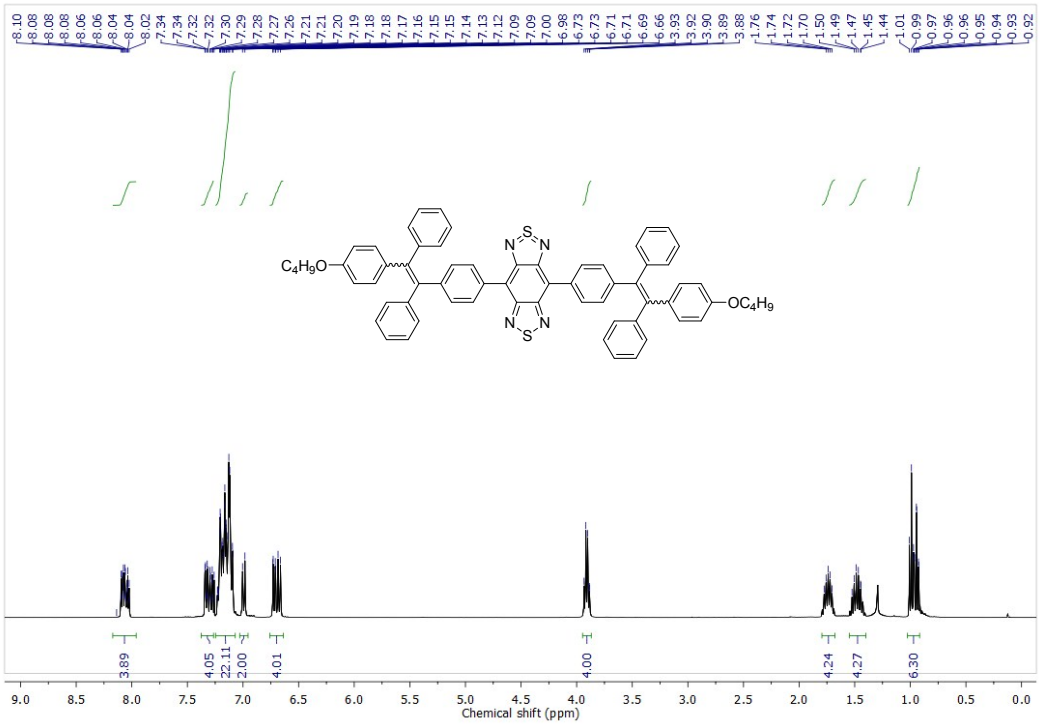

Fig. S8 ^{1}H NMR spectrum of *β*-DTPEBBTD-C4 in $CDCl_3$.

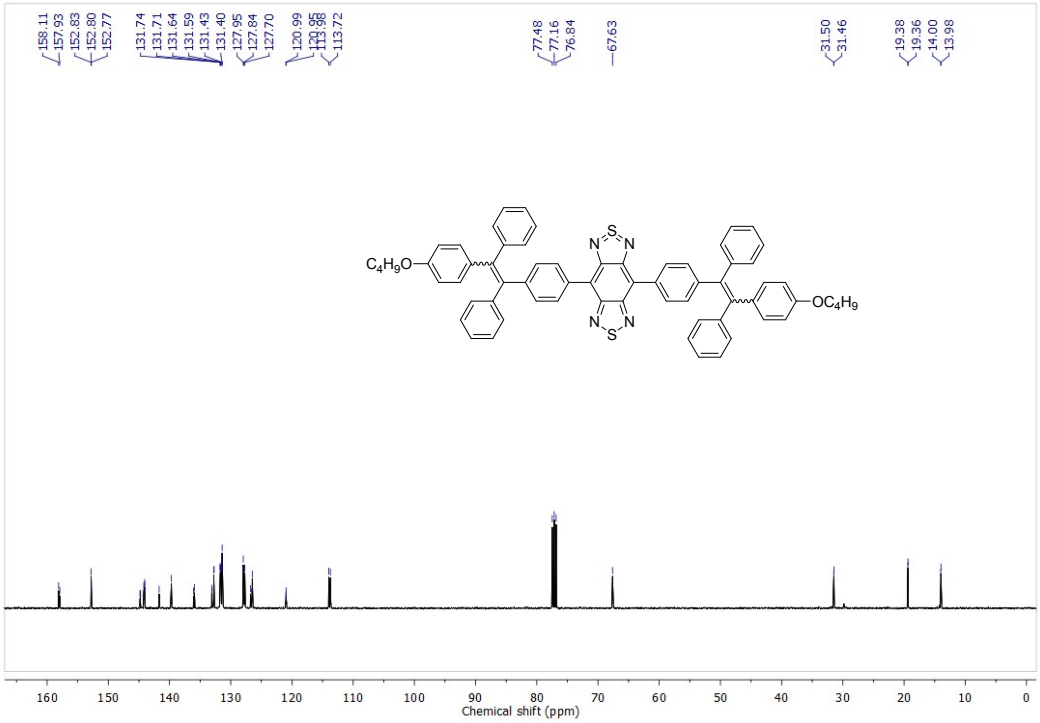

Fig. S9 ^{13}C NMR spectrum of *β*-DTPEBBTD-C4 in $CDCl_3$.

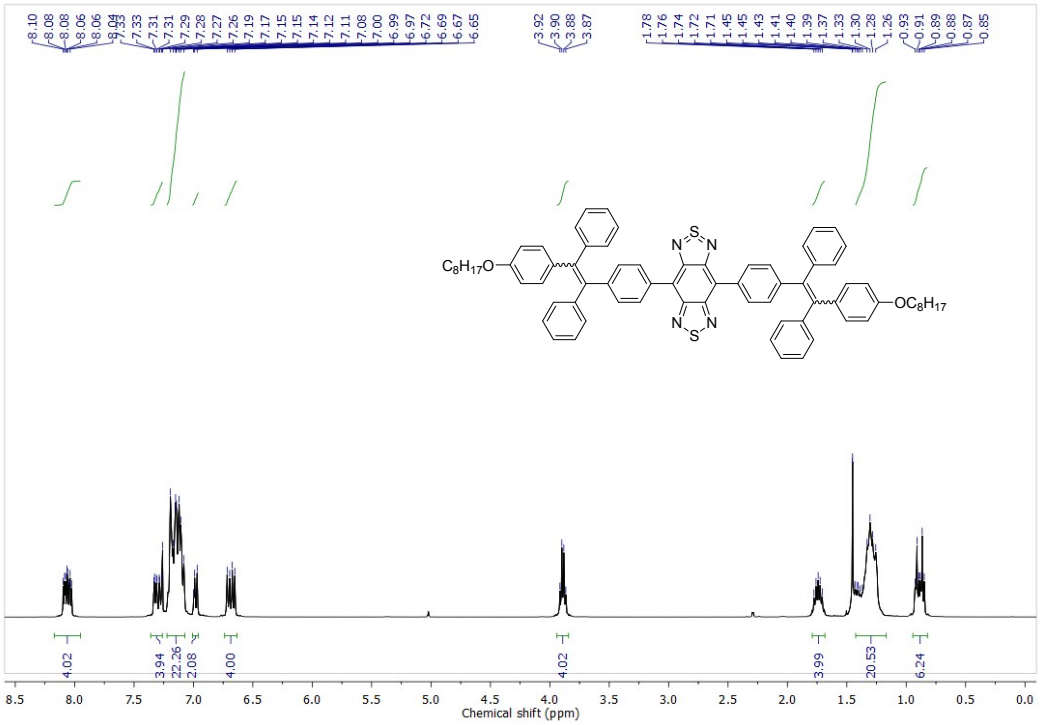

Fig. S10 ^{1}H NMR spectrum of *β*-DTPEBBTD-C8 in $CDCl_3$.

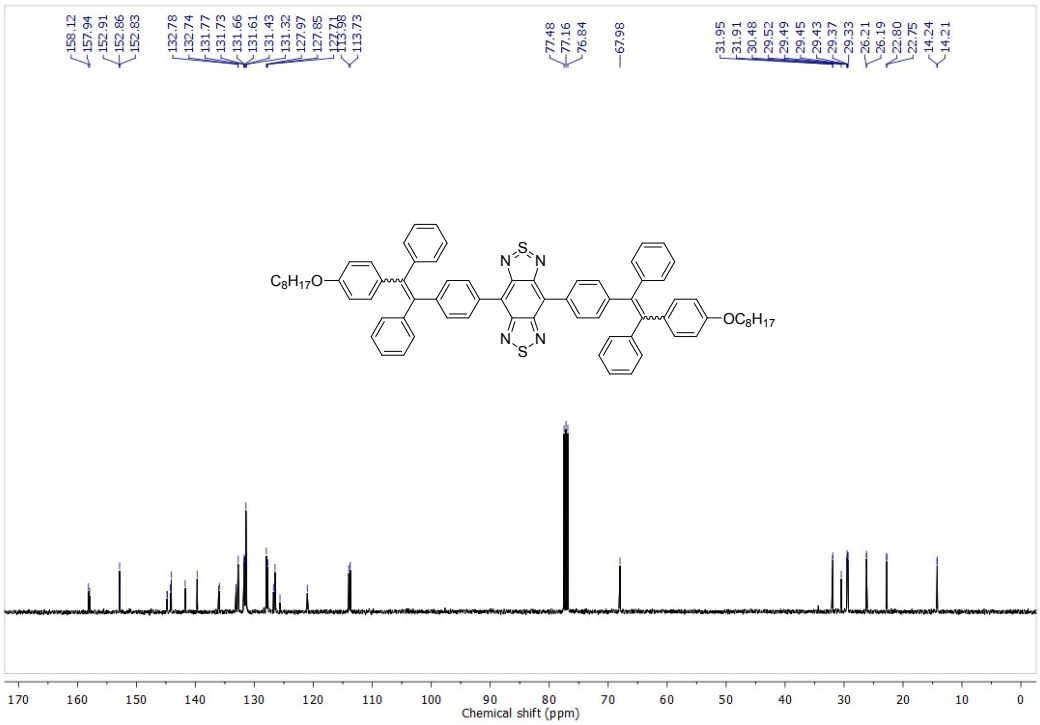

Fig. S11 ^{13}C NMR spectrum of β-DTPEBBTD-C8 in $CDCl_3$.

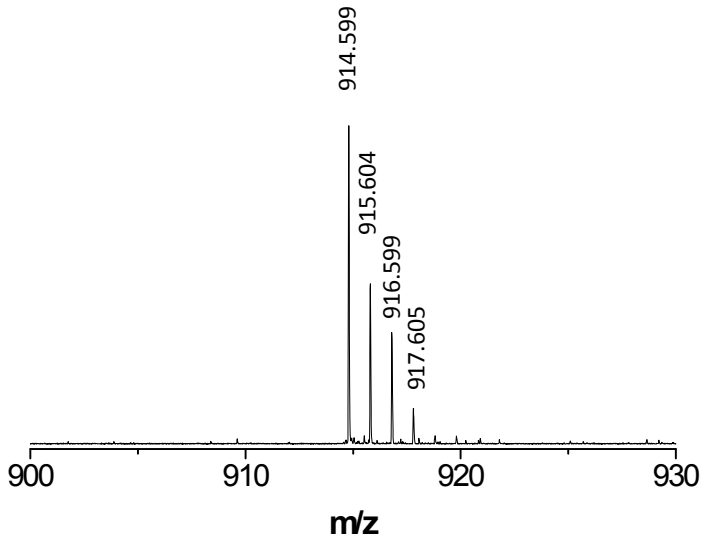

Fig. S12 MALDI-TOF-MS spectrum of α-DTPEBBTD-C1.

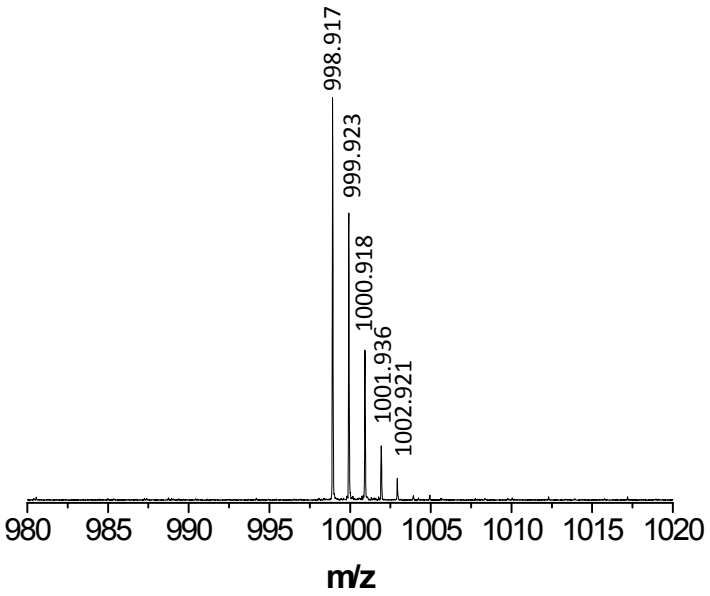

Fig. S13 MALDI-TOF-MS spectrum of α -DTPEBBTD-C4.

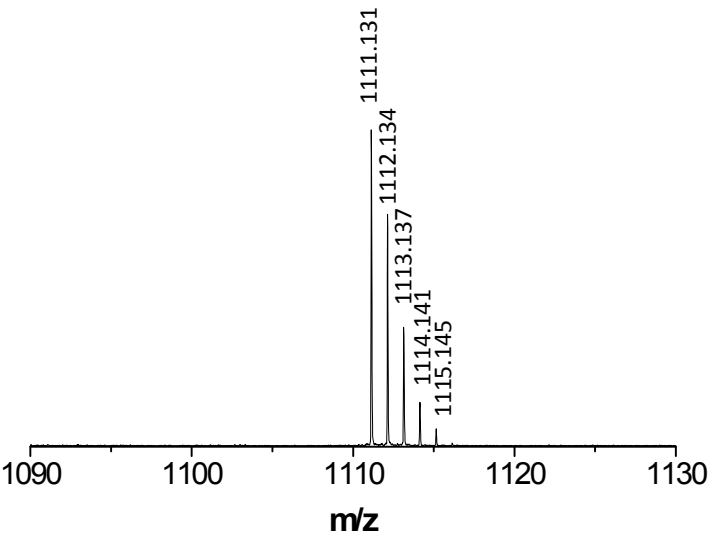

Fig. S14 MALDI-TOF-MS spectrum of α -DTPEBBTD-C8.

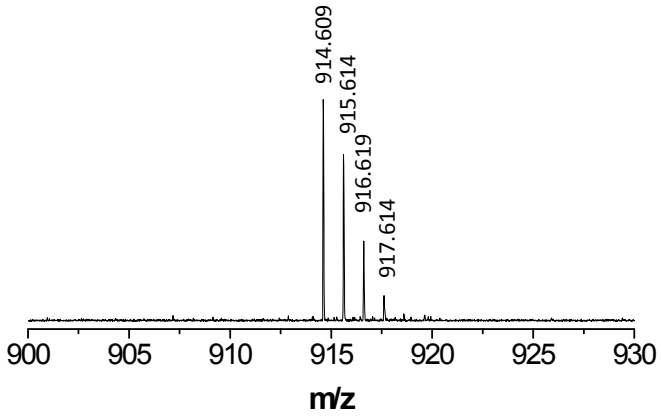

Fig. S15 MALDI-TOF-MS spectrum of *β*-DTPEBBTD-C1.

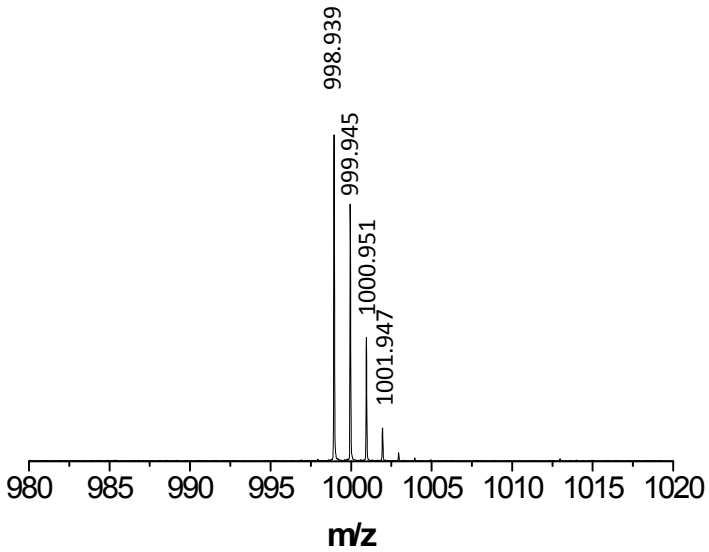

Fig. S16 MALDI-TOF-MS spectrum of *β*-DTPEBBTD-C4.

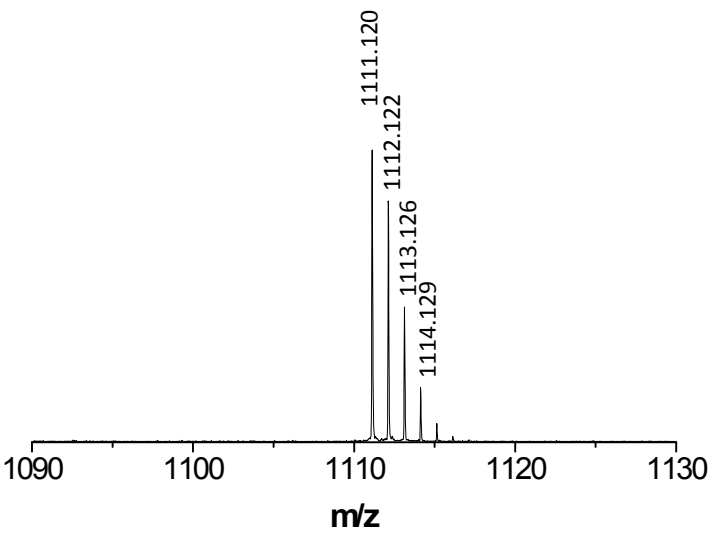

Fig. S17 MALDI-TOF-MS spectrum of *β*-DTPEBBTD-C8.

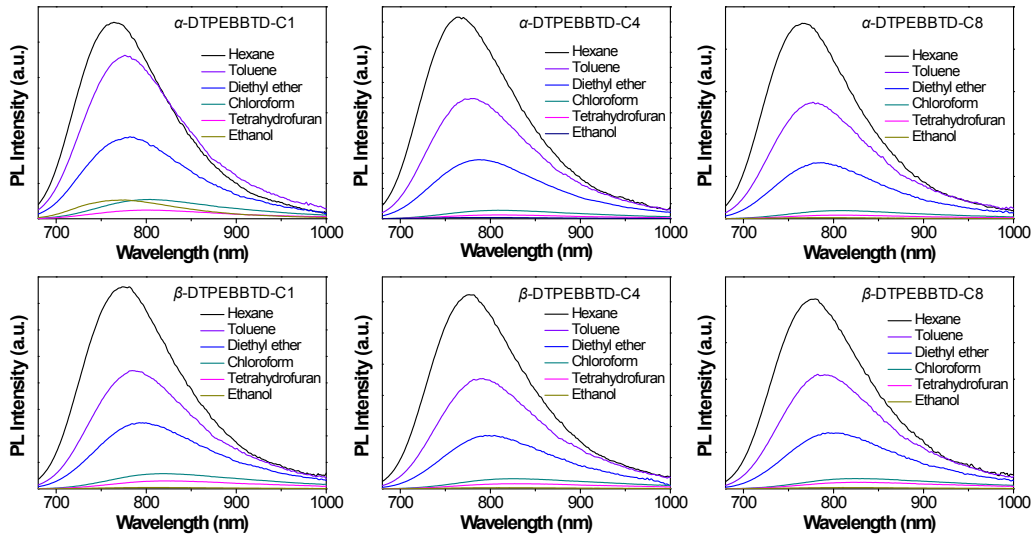

Fig. S18 PL spectra of *α*-DTPEBBTD-Cx and *β*-DTPEBBTD-Cx in different solvents. The PL spectra were collected upon excitation at corresponding absorption maxima. No PL signal was detected in acetonitrile and DMF.

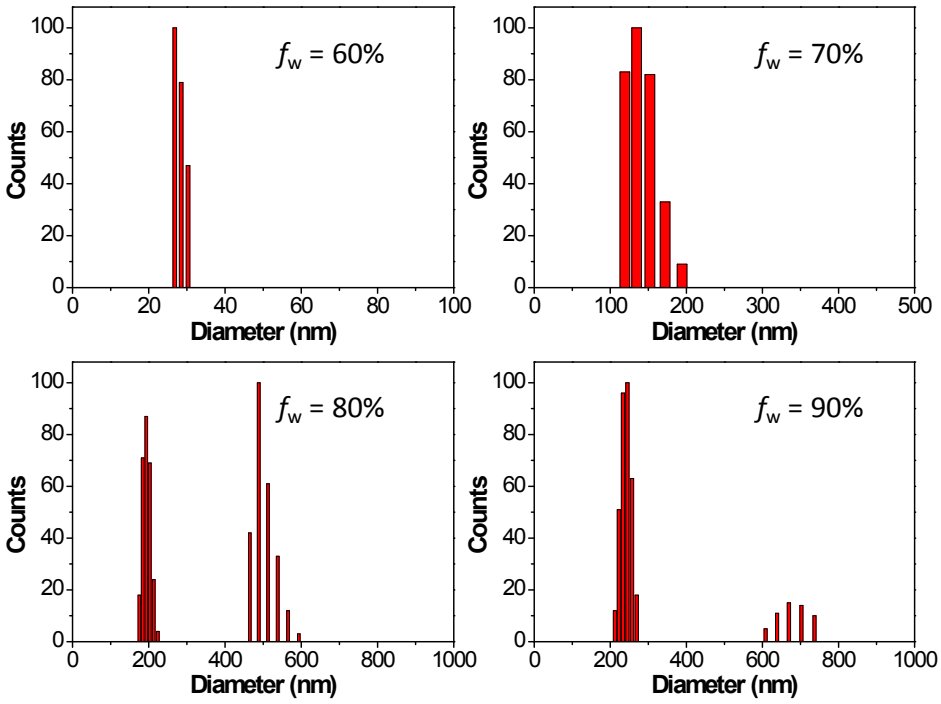

Fig. S19 The LLS results of *β*-DTPEBBTD-C1 in THF/H_2O mixtures with varying volume fractions of water (f_w). No signal was detected when f_w is less than 60%, indicative of no detectable nanoparticles formed.

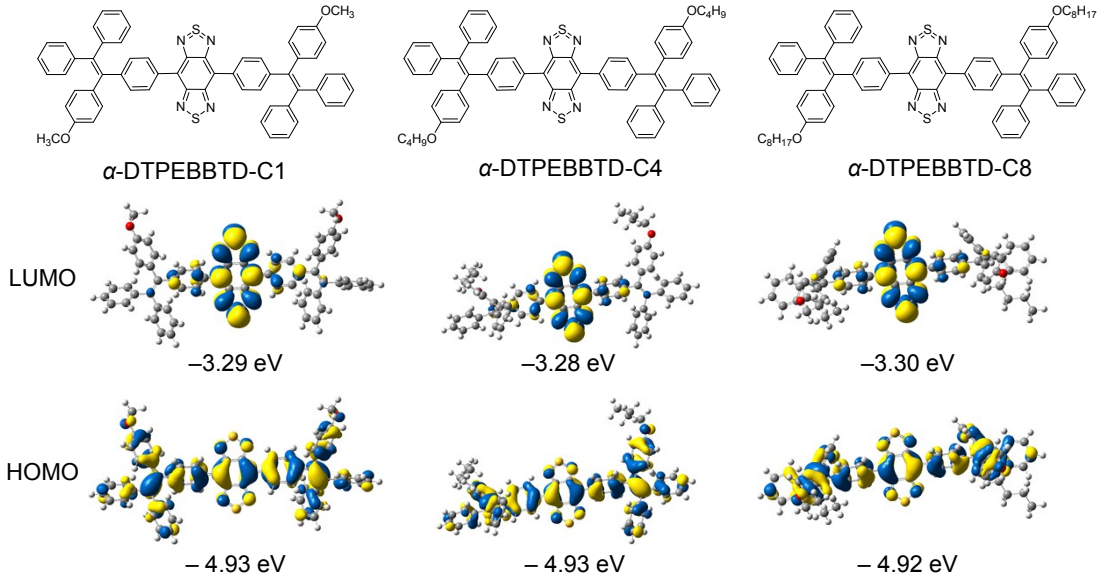

Fig. S20 Calculated molecular orbitals of *α*-DTPEBBTD-C1, *α*-DTPEBBTD-C4 and *α*-DTPEBBTD-C8.

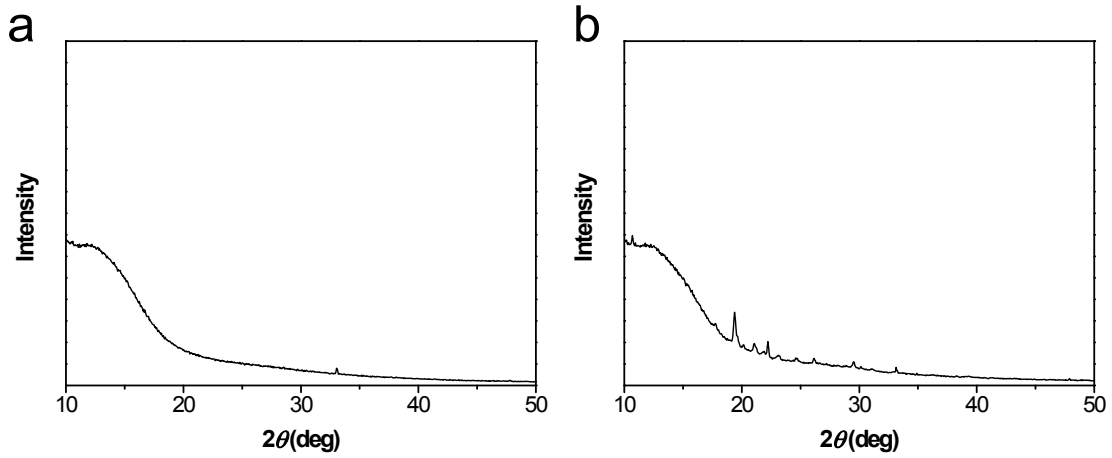

Fig. S21 X-ray diffraction patterns of α-DTPEBBTD-C1 (a) and β-DTPEBBTD-C1 (b).

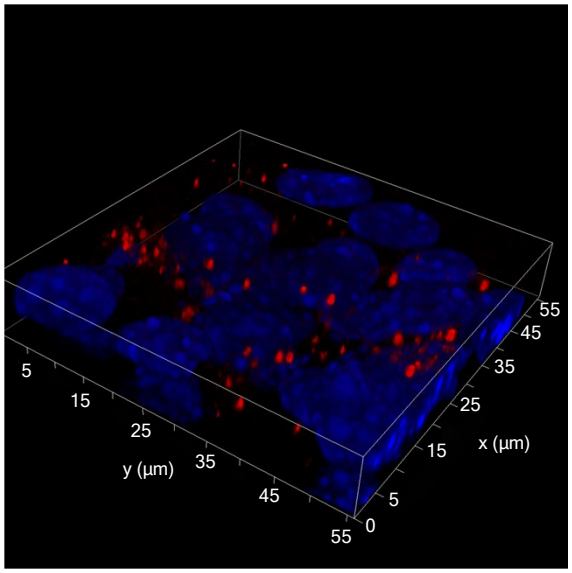

Fig. S22 3D confocal image of 4T1 breast cancer cells after incubation with AIE NPs (2 nM) for 2 h at 37 °C.

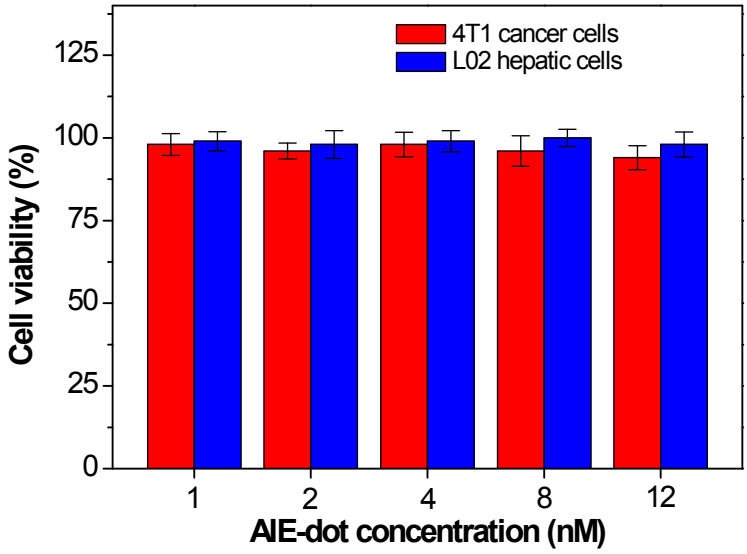

Fig. S23 Cytotoxicity evaluation by MTT assays. Cell viabilities of 4T1 cancer cells and L02 hepatic cells (normal cells) after incubation with α-DTPEBBTD based AIE NPs at different concentrations for 48 h, respectively.

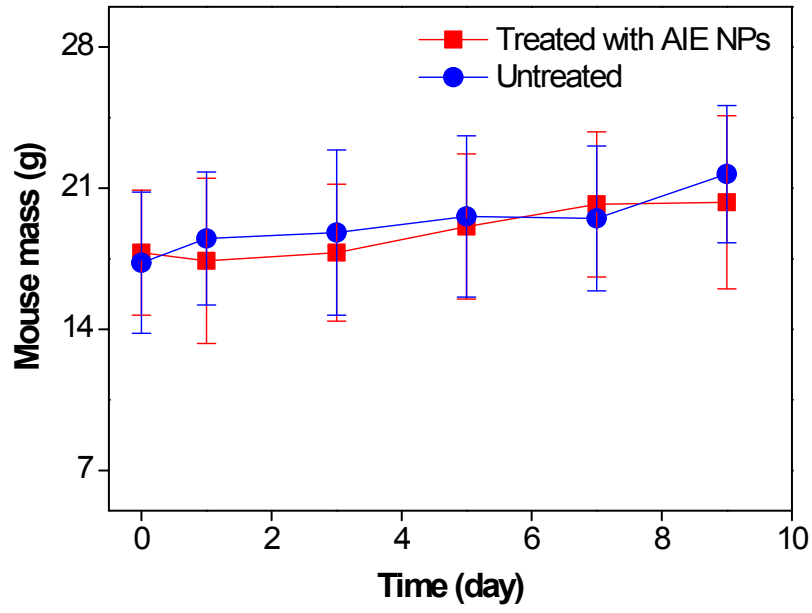

Fig. S24 Body weight changes of mice with and without intravenous injection of α-DTPEBBTD-C4 based AIE NPs (n = 4 per group).

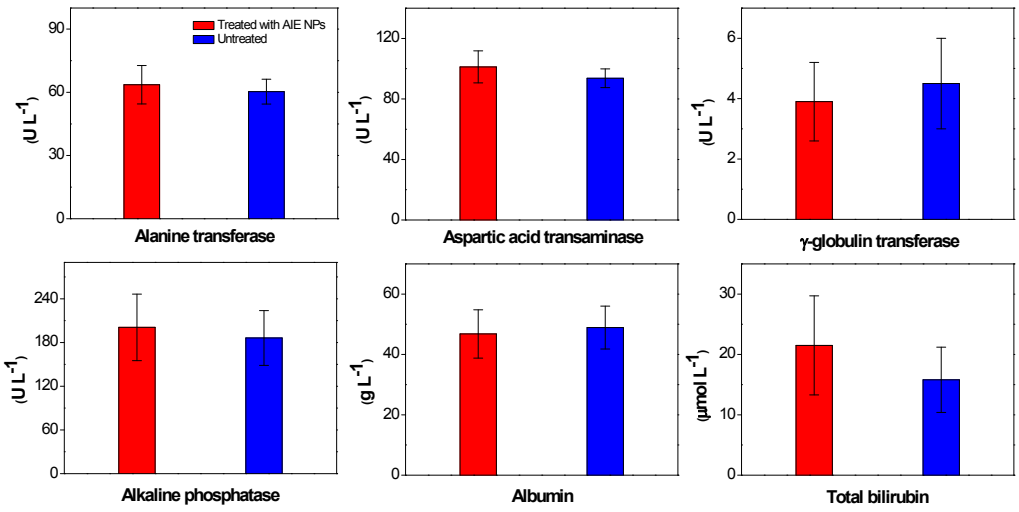

Fig. S25 Blood test parameters regarding liver functions of the mice with and without intravenous injection of α-DTPEBBTD-C4 based AIE NPs (n = 4 per group).

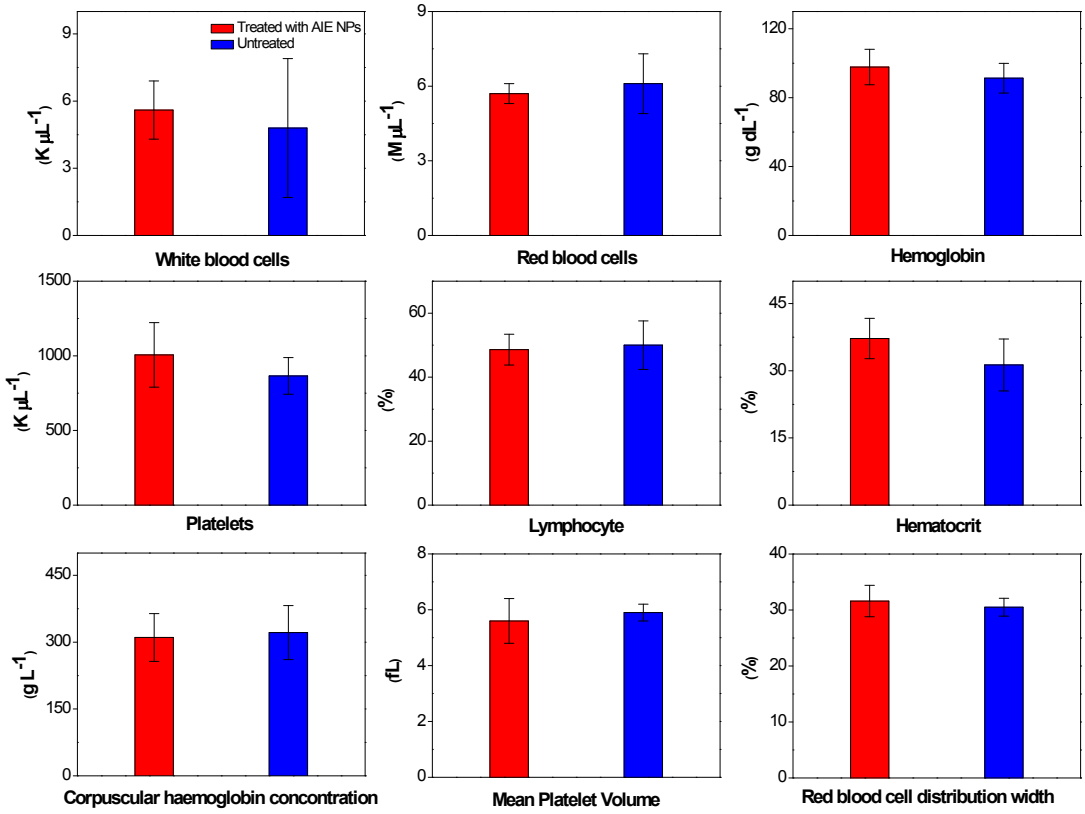

Fig. S26 Blood test parameters regarding white blood cells, red blood cells and haem regulation of the mice with and without intravenous injection of α-DTPEBBTD-C4 based AIE NPs (n = 4 per group).

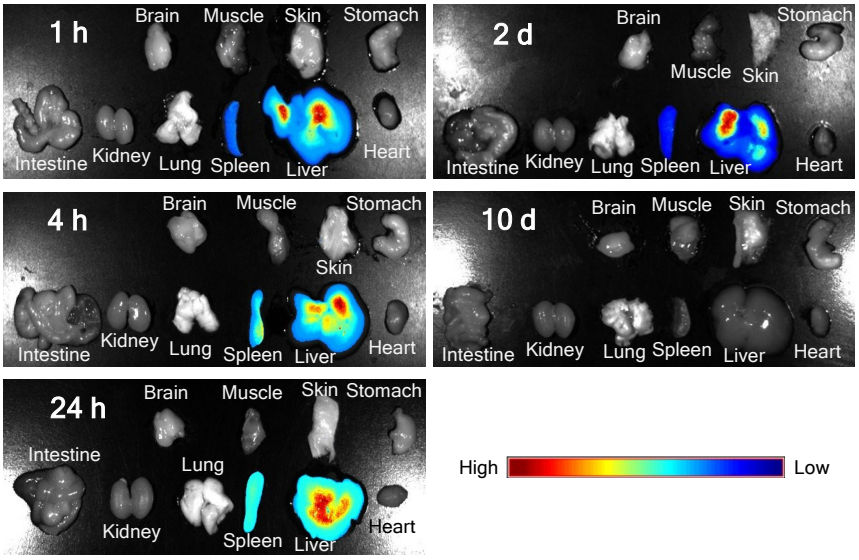

Fig. S27 The ex vivo fluorescence images of the internal organs of mice sacrificed at different periods of time (1 h, 4 h, 24 h, 2 days and 10 days) post-injection with α-DTPEBBTD-C4 based AIE NPs.

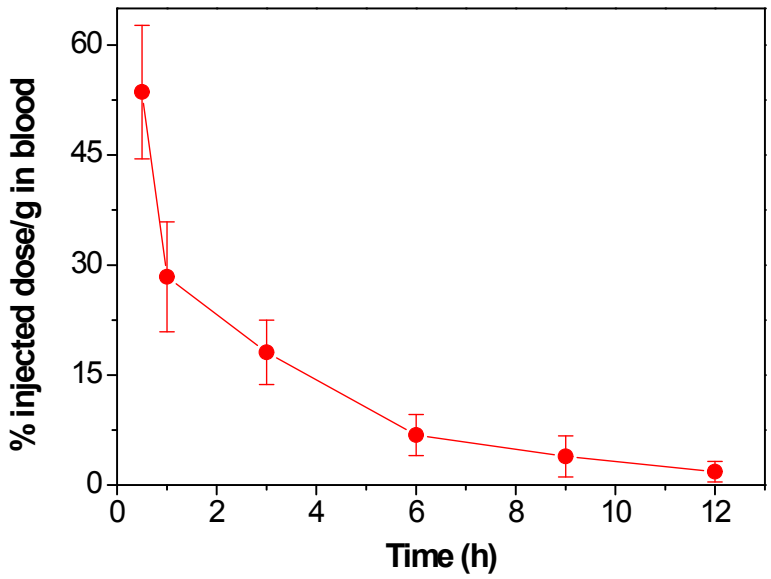

Fig. S28 Blood circulation curve of *α*-DTPEBBTD-C4 based AIE NPs in mice.

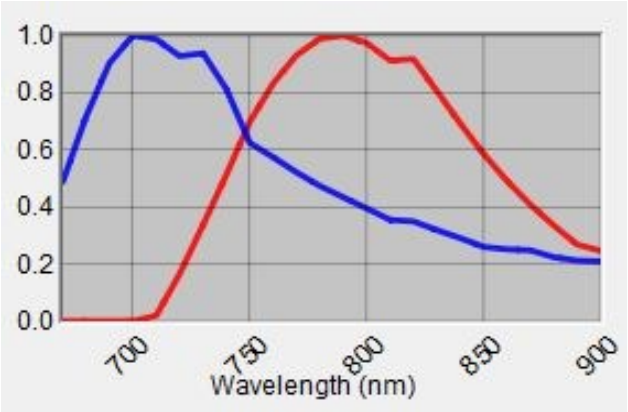

Fig. S29 Spectra of *α*-DTPEBBTD-C4 based AIE NPs fluorescence (red) and mouse autofluorescence (blue) generated by the spectral unmixing function of Maestro software.

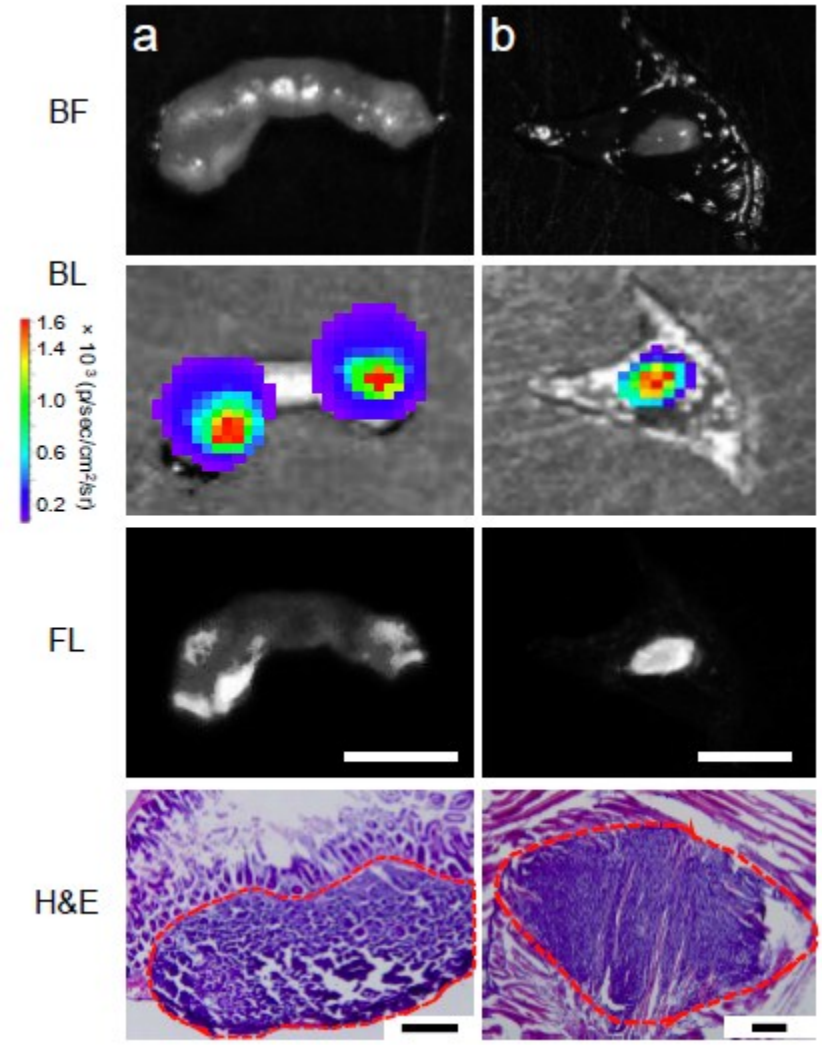

Fig. S30 Hematoxylin and eosin (H&E) histological analyses for the excised intestine and peritoneum. Typical bright field (BF), bioluminescence (BL), fluorescence (FL), and H&E-stained images of (**a**) intestine and (**b**) peritoneum from peritoneal carcinomatosis-bearing mice. *α*-DTPEBBTD-C4 based AIE NPs were intravenously injected into the tumor-bearing mice, which were followed by tissue imaging at 24 h post-injection. The red circles in H&E-stained images indicate tumors infiltrated into surrounding normal tissues. The scale bar represents 4 mm and 250 μm for the FL and H&E-stained images, respectively.

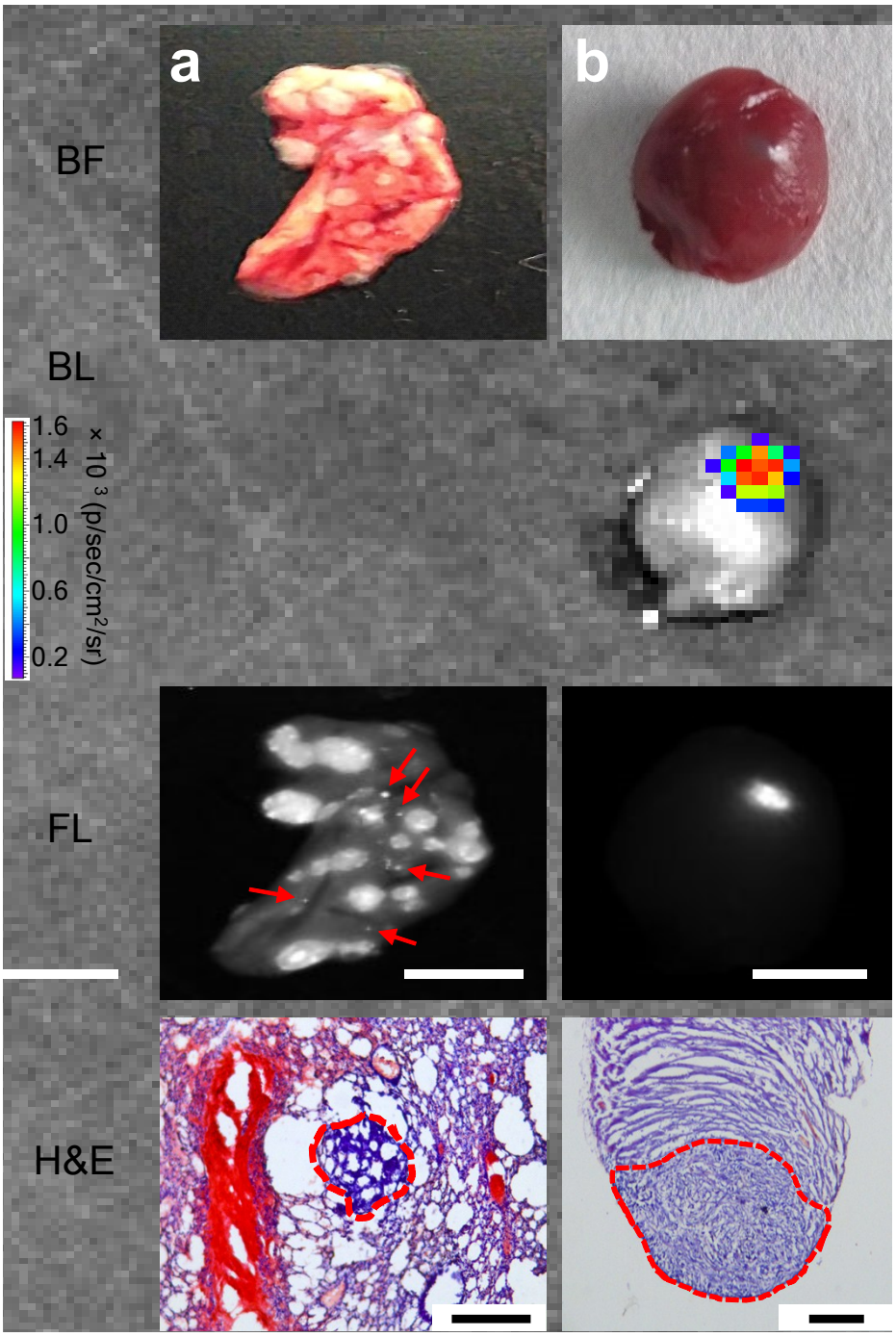

Fig. S31 Hematoxylin and eosin (H&E) histological analyses for the excised lung and heart from mice with lung metastasis of carcinoma. Typical bright field (BF), bioluminescence (BL), fluorescence (FL), and H&E-stained images of (**a**) lung and (**b**) heart from lung metastasis of carcinomatosis-bearing mice. *α*-DTPEBBTD-C4 based AIE NPs were intravenously injected into

the tumor-bearing mice, which were followed by tissue imaging at 24 h post-injection. The red arrows in the FL image of (a) indicate the submillimeter tumors in lung. The red circles in H&E-stained images indicate tumors infiltrated into surrounding normal tissues. The scale bar represents 4 mm and 250 μm for the FL and H&E-stained images, respectively.